PERGAMON

Journal of Quantitative Spectroscopy & Radiative Transfer 72 (2002) 677–689

Journal of Quantitative Spectroscopy & Radiative Transfer

www.elsevier.com/locate/jqsrt

The realization of Abel's inversion in the case of discharge with undetermined radius

Lj.M. Ignjatović*, A.A. Mihajlov

Institute of Physics, P.O. Box 68, Pregrevica 118, 11080 Zemun, Belgrade, Yugoslavia

Received 3 January 2001; accepted 16 March 2001

Abstract

A new method for the determination of the local plasma emissivity on the basis of measuring of the radiation intensity is presented. The method is related to the axial symmetric discharges with undefined radius (free burning arcs, etc.). In this method, the experimental profile of the radiative intensity is approximated by the linear combination of Gaussian functions, while the requested plasma emissivity is obtained in a similar oblique. The essence of the presented method lies in the procedure of determination of the coefficients in this linear combinations, as well as the parameters by which the exponents of Gaussian functions are expressed. The method was tested on a large number of examples which are related to almost all practically important cases of the profiles of local plasma emissivity. It was shown that the method works with high precision, which makes it a certain tool for an operative laboratorial application. © 2002 Elsevier Science Ltd. All rights reserved.

Keywords: Discharge; Undefined radius; Abel's inversion; Measured intensity; Local emissivity

1. Introduction

In this paper, we consider the problem of determination of the local plasma emissivity on the basis of data related to intensity of emitted radiation. We will assume that observed plasma, originated by a gaseous discharge with cylindrical symmetry, can be treated as optically thin. The local plasma emissivity is denoted by $\varepsilon(r)$, where r is the distance from the symmetry axis of discharge.

Usually, considered in the literature is the case where the observed plasma is located inside a cylindrical area with radii R, i.e. when $\varepsilon(r) = 0$ for $r \geqslant R$. The cross section of such discharge is shown in Fig. 1, where the symmetry axis of the observed discharge is taken as the z-axis of

* Corresponding author. Fax: +381-11-3162-190.
E-mail address: ljuba@phy.bg.ac.yu (Lj.M. Ignjatović).

PII: S0022-4073(01)00149-2

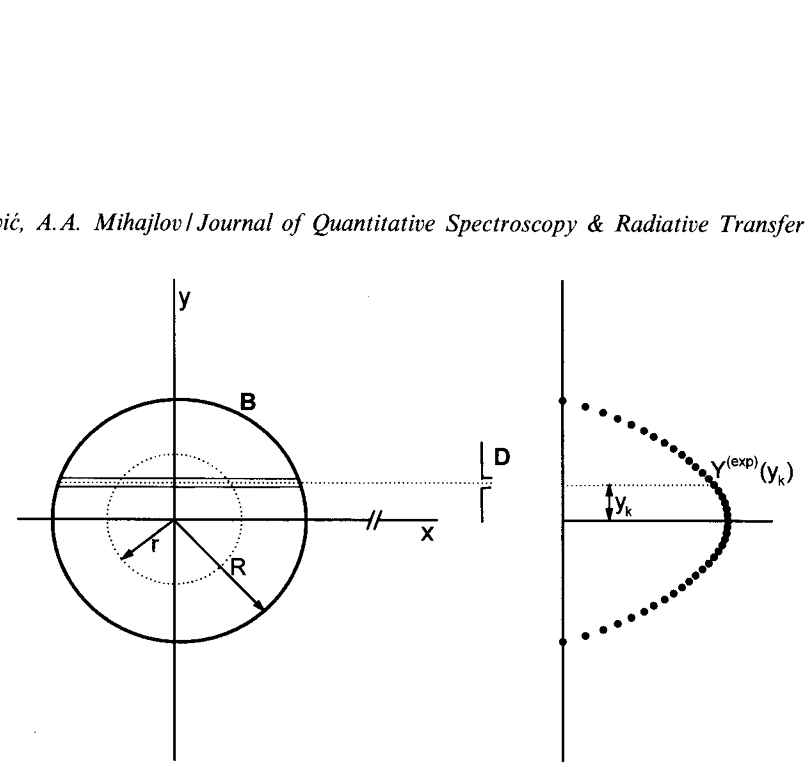

Fig. 1. Experimental set-up in the case of discharges with defined radius (R). Right hand side of the figure shows the profile of measured intensity $Y^{(\mathrm{exp})}$, with which Abel's inversion procedure starts. B—discharge border. D—detector.

the Descartes originated system, the direction toward the detector of emitted radiation is taken as the x-axis, and direction wherein scanning of the discharge is performed as the y-axis. It is assumed that the distance between the z-axis and detector has to be much larger than the discharge radius R. In this figure, as well as in whole paper, $Y^{(\mathrm{exp})}$ denotes the experimental values of the quantity $Y(y)$, which is proportional to the radiation intensity, and which is given by relations

$$Y(y) = \int_{-X(y)}^{X(y)} \varepsilon(r(x, y))\,\mathrm{d}x, \quad r(x, y) = \sqrt{x^2 + y^2}, \tag{1}$$

where $X(y) = \sqrt{R^2 - y^2}$. From here it follows that in the case when $\varepsilon(r \geqslant R) = 0$ the function $Y(y) = 0$ for $y \geqslant R$. Since the proportionality coefficient, which connects the real radiation intensity with this function does not play any role in further considerations, we will treat just $Y(y)$ as the radiation intensity, as it is usual in the literature. Accordingly, the values of the quantity $Y^{(\mathrm{exp})}$ will be treated as values of measured radiation intensity. Hence, the problem which is considered here reduces at determination of the profile of local emissivity $\varepsilon(r)$ on the basis of the given data $Y^{(\mathrm{exp})}$.

In the case of discharges with defined radius the described problem is usually solved with the help of a procedure based on Abel's inversion [1,2]. In this procedure $Y(y)$ is given by the expression

$$Y(y) = 2 \int_y^R \frac{\varepsilon(r) r\,\mathrm{d}r}{\sqrt{r^2 - y^2}}, \tag{2}$$

which is equivalent to (1), and emissivity $\varepsilon(r)$ is obtained afterwards in oblique

$$\varepsilon(r) = -\frac{1}{\pi} \int_r^R \frac{\mathrm{d}Y(y)}{\mathrm{d}y} \frac{\mathrm{d}y}{\sqrt{y^2 - r^2}}. \tag{3}$$

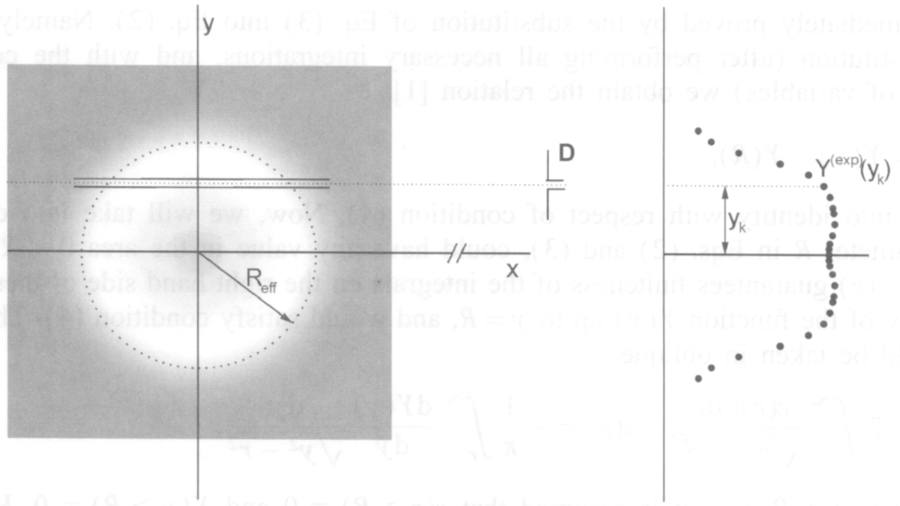

Fig. 2. Same as Fig. 1, but in the case of discharge with undefined radius.

As one can see from these equations, the parameter R plays the essential role and it has the sense of given discharge radii. However, one should have in mind such situations wherein precise determination of this parameter could be connected with some difficulties. Such situations are possible, above all, in the case of discharges which are free burning in the atmosphere of some gas. The same situations are also possible, in the case of discharges which are stabilized by walls, but where a wide intermediate layer exists near the wall, as well as in the case of discharges which are burning in electrolytes. It is clear that in all such situations it would be desirable to have a method wherein such parameter does not exist.

The exact aim of this paper is the presentation of such a method. The method is applicable in the cases when the distance between discharge axis and radiation detector is much larger than some effective radius R_{eff}, so that the contribution of the area $r > R_{eff}$ to the measured radiation intensity can be fully neglected. In fact, the surface radius R_{eff} is somewhere in the bordering layer, where the local emissivity decreases down to negligible level, as Fig. 2 illustrates.

The proposed method, of course, can be applied in the case when the conditions of experiment allow determination of the parameter R. However, in this case (when the radius R automatically takes the role of R_{eff}), presented method can be of interest as an alternative to the methods which are known from the literature [2], because it is not based on the standard polynomial approximation of the functions $Y(y)$, but on using Gaussian functions basis set.

2. Theory

We will start our consideration with the observation that $\varepsilon(r)$, in oblique (3), presents the local emissivity only if $Y(R)$ satisfies the boundary condition

$$Y(R) = 0, \qquad (4)$$

which is immediately proved by the substitution of Eq. (3) into Eq. (2). Namely, as a result of such substitution (after performing all necessary integrations, and with the corresponding replacement of variables) we obtain the relation [1]:

$$Y(y) = Y(y) - Y(R), \tag{5}$$

which turns into identity with respect of condition (4). Now, we will take into consideration that the parameter R in Eqs. (2) and (3), could have any value in the area $0 < R \leqslant \infty$, if the behaviour of $\varepsilon(r)$ guarantees finiteness of the integrals on the right hand side of these equations, the continuity of the function $Y(y)$ up to $y = R$, and would satisfy condition (4). Then, Eqs. (2) and (3) could be taken in oblique

$$Y(y) = 2\int_y^\infty \frac{\varepsilon(r) r\,\mathrm{d}r}{\sqrt{r^2 - y^2}}, \quad \varepsilon(r) = -\frac{1}{\pi}\int_r^\infty \frac{\mathrm{d}Y(y)}{\mathrm{d}y}\frac{\mathrm{d}y}{\sqrt{y^2 - r^2}}, \tag{6}$$

because in the case $R < \infty$ it is assumed that $\varepsilon(r \geqslant R) \equiv 0$ and $Y(y \geqslant R) \equiv 0$. However, for us it is the essential fact that just Eq. (6) made possible the application of Abel's inversion in the case of gaseous discharges which have not exactly determined bordered surface, because such discharges could not be determined by Eqs. (2) and (3), in principle. One should have in mind that the function $\varepsilon(r)$, beside the above mentioned conditions which are necessary for the formal mathematical correctness of Eq. (6), has to satisfy one more condition which is necessary because of physical reasons. Namely, the function $\varepsilon(r)$ has to decrease down to the neglected level inside the area with radius (R_{eff}), which is much smaller than the distance between discharge symmetry axis and radiation detector.

Let us notice that Eq. (6) can be shown in oblique

$$Y(y) = \int_{y^2}^\infty \frac{\varepsilon(r)\,\mathrm{d}(r^2)}{\sqrt{r^2 - y^2}}, \quad \varepsilon(r) = -\frac{1}{\pi}\int_{r^2}^\infty \frac{\mathrm{d}Y(y)}{\mathrm{d}(y^2)}\frac{\mathrm{d}(y^2)}{\sqrt{y^2 - r^2}}, \tag{7}$$

if we replace the variables y and r by y^2 and r^2, taking into account relation $\mathrm{d}Y/\mathrm{d}y = \mathrm{d}Y/\mathrm{d}(y^2)\cdot 2y$. The oblique of these equations suggests that the functions $Y(y)$ and $\varepsilon(r)$ are treated here as functions of y^2 and r^2, respectively. We will have in mind this fact, keeping the same denotation for these functions. We will rewrite Eq. (7) in the form

$$Y(y) = 2\int_0^\infty \varepsilon(r)\,\mathrm{d}(\sqrt{r^2 - y^2}), \quad \varepsilon(r) = -\frac{2}{\pi}\int_0^\infty \frac{\mathrm{d}Y(y)}{\mathrm{d}(y^2)}\mathrm{d}(\sqrt{y^2 - r^2}). \tag{8}$$

Let us remember that $r^2 - y^2 = x^2$ and $\mathrm{d}(\sqrt{r^2 - y^2}) = \mathrm{d}x$. This, with regard to the structure of Eq. (8), suggests that y^2 should be taken in oblique: $y^2 = s^2 + r^2$, where s is a new variable. Accordingly, we can take $\mathrm{d}(\sqrt{y^2 - r^2}) = \mathrm{d}s$, later Eq. (8) obtains the following oblique

$$Y(y) = \int_{-\infty}^\infty \varepsilon(r(x, y))\,\mathrm{d}x, \tag{9}$$

$$\varepsilon(r) = \int_{-\infty}^\infty \left(-\frac{1}{\pi}\right)\frac{\mathrm{d}Y(y(s, r))}{\mathrm{d}(s^2)}\,\mathrm{d}s, \tag{10}$$

if we take into account that $\mathrm{d}Y/\mathrm{d}(y^2) = \mathrm{d}Y/\mathrm{d}(s^2)$. Just the system of coupled Eqs. (9) and (10) is the base for our further considerations.

Now, we will call our attention to the fact that one of the solutions follows directly from the form of this system, if one takes $Y(y) = Y^{(0)}(y)$, where $Y^{(0)}(y) = C^{(0)}\exp(-\pi y^2)$ satisfies the differential equation

$$-\frac{1}{\pi}\frac{\mathrm{d}Y(y)}{\mathrm{d}(s^2)} = Y(y). \tag{11}$$

At first, with respect to the relation $y^2 = s^2 + r^2$, from Eq. (10) it follows that in this case the corresponding local emissivity is obtained in oblique $\varepsilon^{(0)}(r) = C^{(0)}\exp(-\pi r^2)$. On the other hand, with respect to relations $\varepsilon(r) = \varepsilon^{(0)}(r)$ and $r^2 = x^2 + y^2$, from Eq. (9) it follows that the corresponding radiation intensity is $Y(y) = Y^{(0)}(y)$. Accordingly, the functions $Y^{(0)}(y)$ and $\varepsilon^{(0)}(r)$ exactly are one of the solutions of system (9) and (10).

The importance of this example is that it brings into consideration the Gaussian functions, having in mind that the corresponding linear combinations of the functions $\exp(-\alpha y^2)$ and $\exp(-\alpha r^2)$, are also possible solutions of system (9) and (10). Here we keep in mind that the linear combinations

$$Y_N(y) = \sum_{n \geqslant 1}^{N} a_n \mathrm{e}^{-\gamma_n y^2}, \tag{12}$$

$$\varepsilon_N(r) = \sum_{n \geqslant 1}^{N} b_n \mathrm{e}^{-\gamma_n r^2}, \quad b_n = a_n \sqrt{\frac{\gamma_n}{\pi}}, \tag{13}$$

where the parameters N and γ_n satisfy the conditions

$$1 \leqslant N < \infty, \quad \gamma_n > 0, \quad \alpha_{n+1} > \gamma_n. \tag{14}$$

The functions $Y_N(y)$ will be used here for the approximation of the experimental radiation intensity, as the linear combinations of the power degree functions are used during Abel's procedure with defined R. Accordingly, in our case the problem reduces to the determination of the coefficients a_n, the parameters γ_n, and the number of Gaussian functions N.

3. Method

From several investigated variants for the determination of the parameters γ_n we chose such ones where γ_n are defined by the relation

$$\gamma_n = \alpha + (n-1)\beta, \quad n = 1, 2, \ldots, N \tag{15}$$

with $\alpha > 0$ and $\beta > 0$. In this manner the problem simplifies, because determination of N parameters γ_n reduces now to the determination of only two parameters: α and β. In accordance with expressions (15), (12) and (13) the functions $Y_N(y)$ and $\varepsilon_N(r)$ can be taken in oblique

$$Y_N(y) = e^{-\alpha y^2} \sum_{n=1}^{N} a_n e^{-(n-1)\beta y^2}, \tag{16}$$

$$\varepsilon_N(r) = e^{-\alpha r^2} \sum_{n=1}^{N} b_n e^{-(n-1)\beta r^2}, \quad b_n = a_n \sqrt{\frac{\alpha + (n-1)\beta}{\pi}}, \tag{17}$$

which is convenient for further considerations.

The determination of the number of Gaussian functions (N), the coefficients a_n, and the parameters α and β is performed here with the help of a procedure which is based on the minimization of the quantity

$$\chi^2_{\{a\}}(N, \alpha, \beta) = \sum_k \left[Y(y_k) - Y_k^{(\exp)} \right]^2, \quad \{a\} \equiv \{a_1, a_2, \ldots, a_N\}, \tag{18}$$

where the summation is performed over all dots $y = y_k$, wherein the experimental values of the radiation intensity $Y_k^{(\exp)}$ were determined. In the frame of this work it is assumed that $-K \leqslant k \leqslant K$, as well as that the experimental profile of the radiation intensity is symmetric with respect to dot $y = 0$. It means $y_{-k} = -y_k$ and $Y_{-k}^{(\exp)} = Y_k^{(\exp)}$. Due to this, in further considerations only the positive wing of this profile ($y_k \geqslant 0$) figures.

First, used procedure assumes that N is being varied with the constant step $\Delta N = 1$ from $N = 1$ to $N = N_{\max}$, while α and β are varied with the corresponding constant steps within the intervals $(\alpha_{\min}, \alpha_{\max})$ and $(\beta_{\min}, \beta_{\max})$, where $\alpha_{\min} > 0$ and $\beta_{\min} > 0$. Second, it is assumed that for each concrete group of values N, α and β, the coefficients a_n are determined by the method of the least squares, i.e. from the condition

$$\frac{\partial(\chi^2_{\{a\}})}{\partial a_n} = 0, \quad 1 \leqslant n \leqslant N, \tag{19}$$

where $Y(y)$ is given by (16).

Regarding the number of Gauss functions N we took the upper boundary $N_{\max} \sim K$. Determining the interval $(\alpha_{\min}, \alpha_{\max})$ we had in mind that, in agreement with the above mentioned, the function $Y_N(y)$ has to decrease rapidly with increasing of y. This condition is satisfied automatically because $\alpha_{\min}$ is taken very close to its approximative value α_0, which is determined from the wing of distribution $Y_k^{(\exp)}$. Namely, it follows from Eqs. (16) and (15) that $Y_N(y)$ asymptotically approaches the function const $\cdot \exp(-\alpha y^2)$. Supposing that the wing of the experimental distribution $Y_k^{(\exp)}$, at least for $k = K$ and $k = K - 1$ is falling into asymptotical region, we can determine approximative value $\alpha = \alpha_0$ directly from the ratio $Y_K^{(\exp)}/Y_{K-1}^{(\exp)}$. Later, it is found that it is enough to vary α from $\alpha_{\min} \cong 0.90\alpha_0$ to $\alpha_{\max} \cong 1.1\alpha_0$, and β—from $\beta_{\min} = 0.5\alpha_0$ to $\beta_{\max} \approx 2\alpha_0$.

Secondly, the procedure presented assumes performing of selection of the functions $Y_N(y)$, which are obtained in manner described above, because between them could appear one such whose behaviour does not satisfy the criteria of physical reasons. Here the following criteria were taken: (1) the functions $Y_N(y)$ and $\varepsilon_N(r)$ have to be positively defined everywhere in the area $y \geqslant 0$ and $r \geqslant 0$, respectively; (2) the absence of the zeroes of derivations $dY_N(y)/dy$ and $d\varepsilon_N(r)/dr$ in the areas $y > y_K$ and $r > y_K$, which provides monotonous decreasing of the functions $Y_N(y)$ and $\varepsilon_N(r)$ in these areas; (3) minimality of the deviation of these functions with respect to the conditions of local monotony, which assumes that in each interval (y_k, y_{k+2}) the function $Y_N(y)$ changes exactly monotonous, if monotonous changing of the values $Y_k^{(\mathrm{exp})}$, $Y_{k+1}^{(\mathrm{exp})}$, $Y_{k+2}^{(\mathrm{exp})}$, and it has only one extremum in all other cases; (4) minimality of the numbers of the extrema of functions $Y(y)$ and $\varepsilon(r)$ in the areas $0 \leqslant y$, $r \leqslant y_K$.

The functions $Y_N(y)$, which satisfy just mentioned criteria, form the group of possible solutions of the considered problem. In the frame of this work, as a final solution $Y^{(\mathrm{fin})}(y)$ is taken as one such from this group, which corresponds to minimal square of the deviation $\chi^2(N, \alpha, \beta)$. The local emissivity, which corresponds to the function $Y^{(\mathrm{fin})}(y)$, and whose determination is our main task, is denoted here as $\varepsilon^{(\mathrm{fin})}(r)$.

4. Results and discussion

The described method was systematically tested on three groups of examples. The first group consisted of examples wherein the local emissivity $\varepsilon(r)$ is a strictly decreasing function of r, the

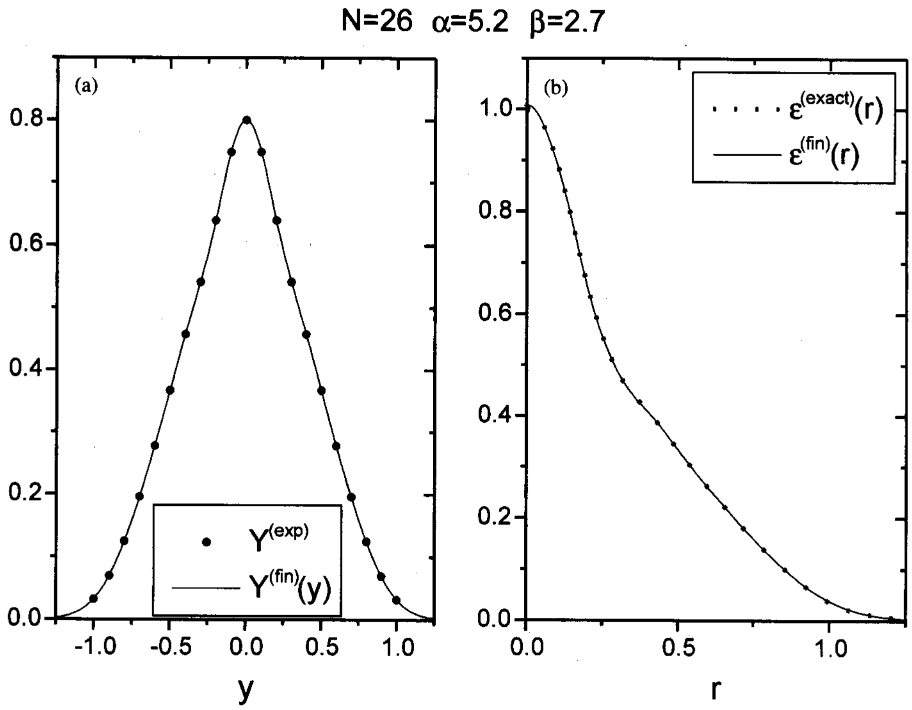

Fig. 3. The discharges with a strictly decreasing radial emissivity distribution (the case of small halfwidth). Part (a): $Y^{(\mathrm{exp})}$—simulated measured intensity, obtained on the base of the local emissivity profile $\varepsilon^{(\mathrm{exact})}(r)$, $Y^{(\mathrm{fin})}(y)$—approximation of measured intensity by final linear combination of Gaussian functions. Part (b): $\varepsilon^{(\mathrm{exact})}(r)$—started local emissivity profile, $\varepsilon^{(\mathrm{fin})}(r)$—local emissivity determined on the base of $Y^{(\mathrm{fin})}(y)$.

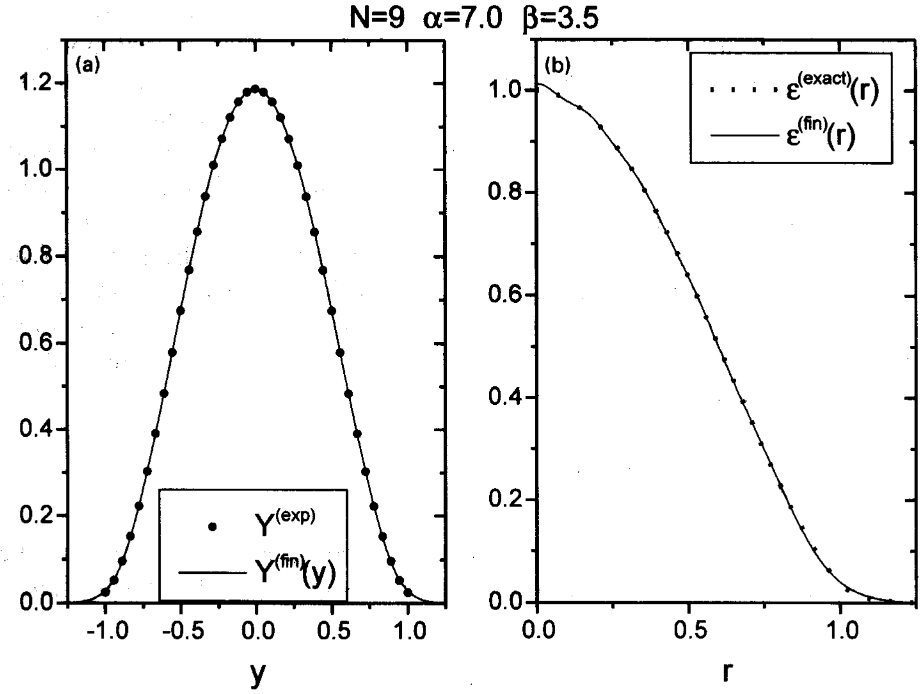

Fig. 4. Same as Fig. 3, but in the case of middle halfwidth of radial emissivity distribution.

second group—examples wherein $\varepsilon(r)$ has a clearly expressed plateau, and the third—examples wherein $\varepsilon(r)$ has the minimum in the centre. For each group the shape of the wing has been varied. Besides, for the first group the halfwidth has been varied, for the second group—the width of plateau, and for the third group—the depth and the width of the minimum.

Each example has been treated in the same manner. We started from nonanalytical profile of the local emissivity, which is given in an array of discrete points, and normalized on unit in $r=0$. Later, on the basis of this profile, we constructed a continual profile $\varepsilon^{(\mathrm{exact})}(r)$ with help of the third order spline. Using expression in Eq. (9), with $\varepsilon(r)=\varepsilon^{(\mathrm{exact})}(r)$, we determined the values of the simulated measured intensity in the dots $y=y_k$, which played the role of the values $Y_k^{(\mathrm{exp})}$. On the so-generated data-set we applied the procedure described above. As a result we have obtained the best approximation (in the above described sense) for the measured intensity $Y^{(\mathrm{fin})}(y)$, as well as the corresponding local emissivity $\varepsilon^{(\mathrm{fin})}(r)$ which was, afterwards, compared with the values $\varepsilon^{(\mathrm{exact})}(r)$.

The results which are obtained are shown in Figs. 3–10. In the parts of these figures denoted by (a), the values of the simulated radiative intensity $Y_k^{(\mathrm{exp})}$ are shown by dots, while the full curve shows $Y^{(\mathrm{fin})}(y)$; in the parts denoted by (b), the profiles $\varepsilon^{(\mathrm{exact})}(r)$ are shown by dashed line, while the full curve shows requested profile $\varepsilon^{(\mathrm{fin})}(r)$. With regard to these figures, let us note that y and r are given in arbitrary units wherein $y_K=1$.

Figs. 3–8 are related to above described three groups of profiles. All figures demonstrate very good agreement of the found profiles $\varepsilon^{(\mathrm{fin})}(r)$ in comparison with $\varepsilon^{(\mathrm{exact})}(r)$. The profiles $\varepsilon^{(\mathrm{fin})}(r)$

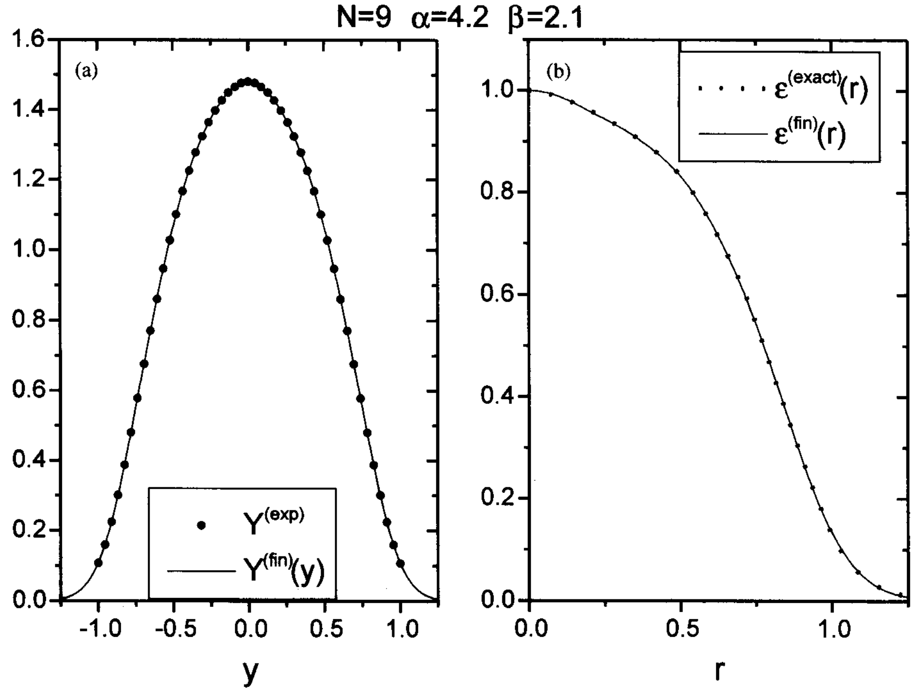

Fig. 5. Same as Fig. 3, but in the case of large halfwidth of radial emissivity distribution.

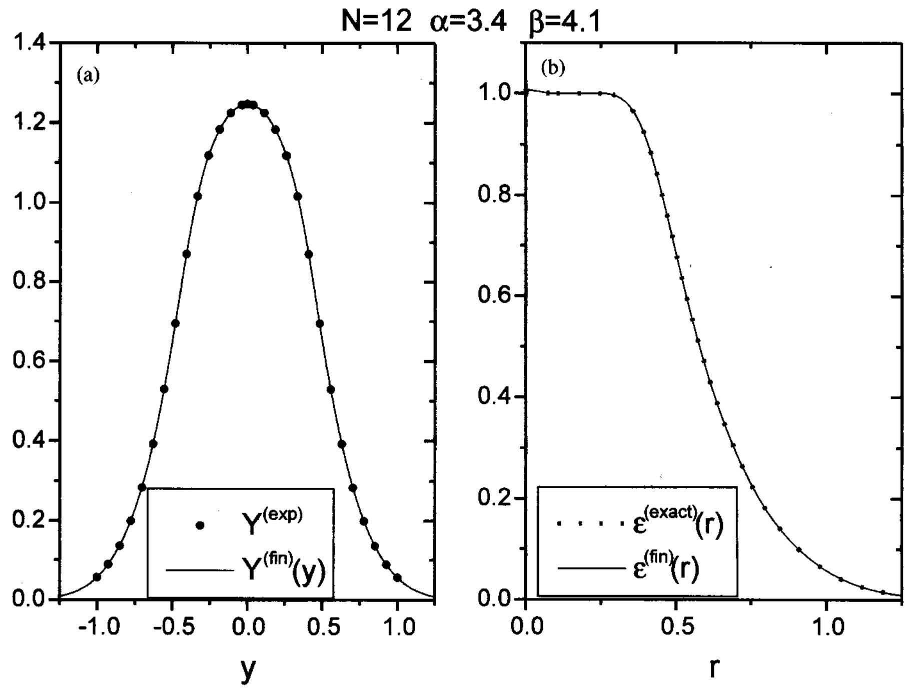

Fig. 6. The discharges with clearly expressed plateau on radial emissivity distribution (the case of narrow plateau). Rest as Fig. 3.

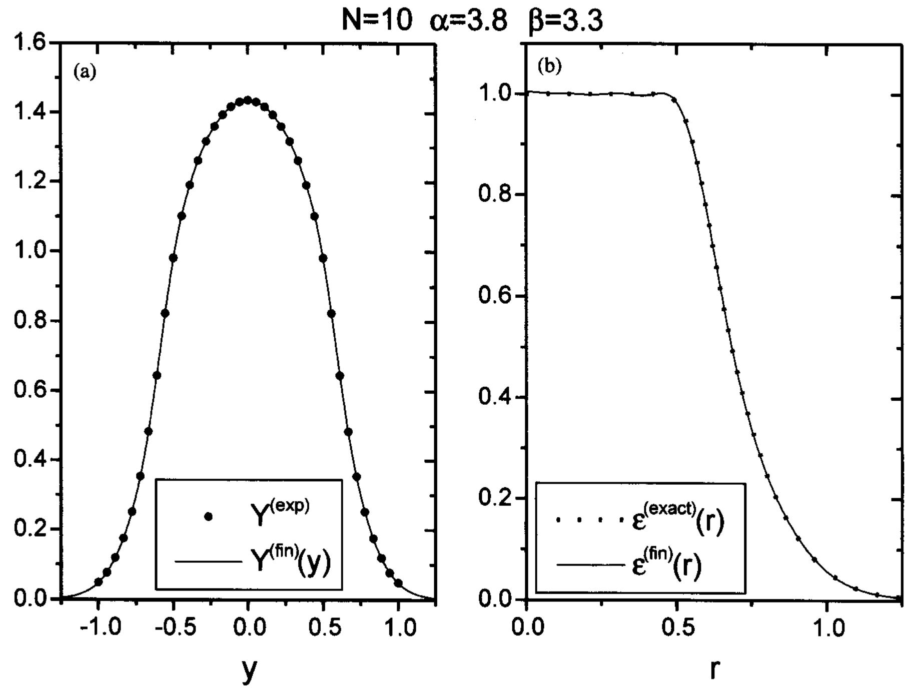

Fig. 7. Same as Fig. 6, but in the case of wide plateau. Rest as Fig. 3.

correspond to the found final values of N, α, and β which are given on these figures. Due to space economizing, only the last example (shown in Fig. 8) is presented together with the corresponding table which makes possible the quantitative analysis. Substituting the necessary data

$$N=10, \quad \alpha=5.2, \quad \beta=4.3,$$

$$a_1=27.18, \quad a_2=-237.04, \quad a_3=1290.54, \quad a_4=-4477.85,$$
$$a_5=10316.96, \quad a_6=-16081.71, \quad a_7=16788.71, \quad a_8=-11236.35,$$
$$a_9=4352.47, \quad a_{10}=-741.06$$

into Eqs. (16), (17), we obtain the functions $Y^{(\mathrm{fin})}(y)$ and $\varepsilon^{(\mathrm{fin})}(r)$ whose values are compared with $Y^{(\mathrm{exp})}$ and $\varepsilon^{(\mathrm{exact})}(r)$ in Table 1.

In order to test the applicability of described method when the profile of the local emissivity is more complicated, we used the data about the radial profile of the density $n(r)$ for one kind of atoms in the gaseous discharges from [3]. Concretely, we took $\varepsilon^{(\mathrm{exact})}(r)=\mathrm{const}\cdot n(r)$, and applied our method. The result is shown in Fig. 9. As one can see an excellent agreement between $\varepsilon^{(\mathrm{fin})}(r)$ and $\varepsilon^{(\mathrm{exact})}(r)$ exists.

At last, in order to test the applicability of our method in the cases which permit to introduce the discharge radius R, we considered examples from [2]. The data for the local emissivity and

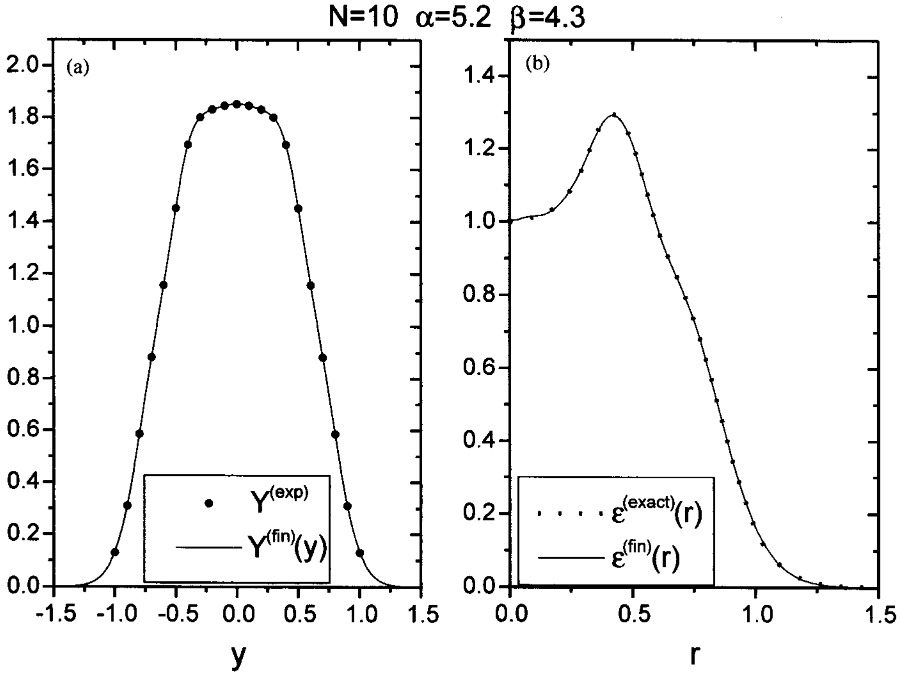

Fig. 8. The discharges with clearly expressed minimum in the centre of radial emissivity distribution. Rest as Fig. 3.

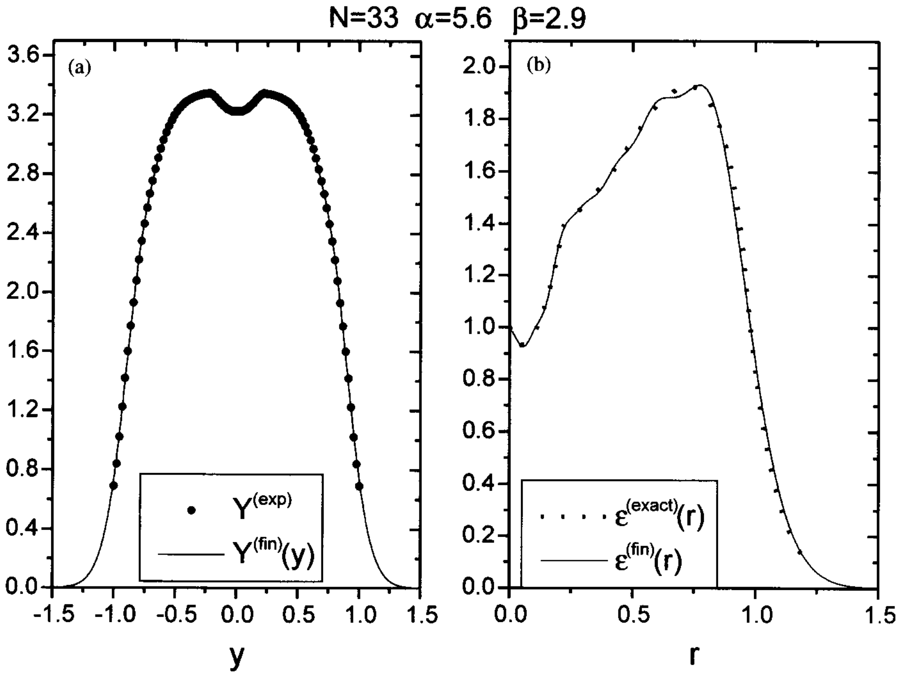

Fig. 9. The discharges with more complicated oblique of radial emissivity distribution. Rest as Fig. 3.

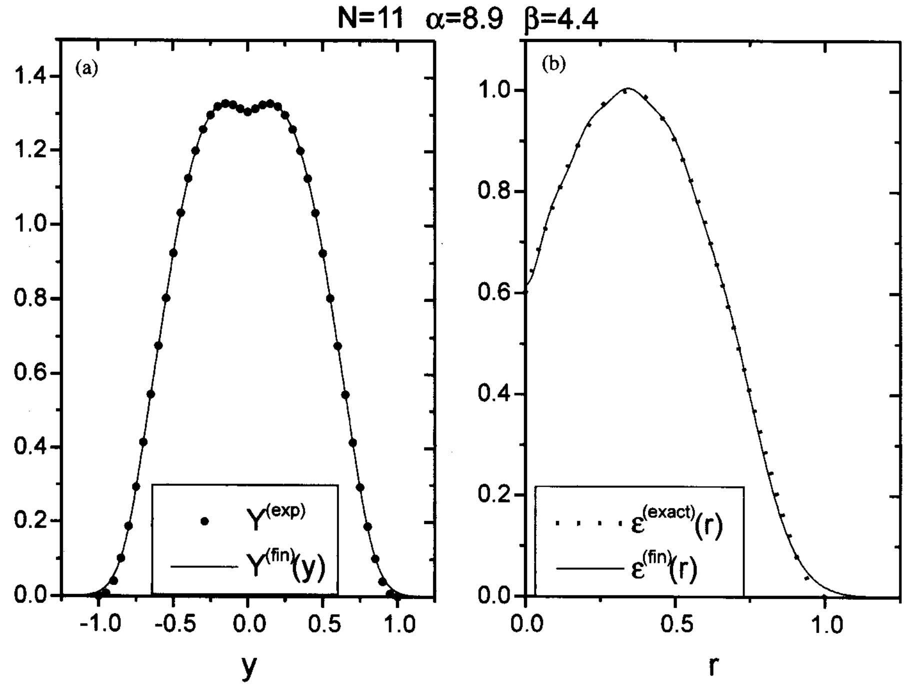

Fig. 10. Application of described method to the case of discharge with defined radius (R). Values $Y^{(\mathrm{exp})}$ are taken from [2], while rest is same as Fig. 3.

Table 1
Quantitative comparison between starting and final values of radial emissivity distribution. Same example is shown in Fig. 8

R	$Y^{(\mathrm{exp})}$	$Y^{(\mathrm{fin})}$	$\varepsilon^{(\mathrm{exact})}$	$\varepsilon^{(\mathrm{fin})}$
0.0	1.8522	1.8500	1.0000	0.9905
0.1	1.8463	1.8456	1.0124	1.0088
0.2	1.8311	1.8322	1.0469	1.0471
0.3	1.8016	1.8024	1.1554	1.1587
0.4	1.6959	1.6956	1.2924	1.2891
0.5	1.4515	1.4519	1.2117	1.2111
0.6	1.1569	1.1574	0.9851	0.9867
0.7	0.8816	0.8814	0.8184	0.8174
0.8	0.5853	0.5847	0.6234	0.6204
0.9	0.3098	0.3111	0.3626	0.3641
1.0	0.1304	0.1334	0.1554	0.1647
1.1		0.0480	0.0610	0.0607
1.2		0.0149	0.0218	0.0191

the radiative intensity were taken as a base, but without the last dots which correspond to the zeroth values of these quantities. The most complicated example, which is characterized by deep minimum in the centre, is shown in Fig. 10.

On the basis of the shown results, it is clear that the presented method can be successfully applied for the diagnostics of the free burning discharges with the most different distributions of the local emissivity. One of its positive features is that $Y^{(\mathrm{fin})}(y)$ and $\varepsilon^{(\mathrm{fin})}(r)$ are obtained in the simple analytical form. Another such feature is the exponential decreasing of the functions $Y^{(\mathrm{fin})}(y)$ and $\varepsilon^{(\mathrm{fin})}(r)$ in the wing areas, which enables that in a usual manner, would determine the effective radius of the free burning discharge R_{eff}. Finally, the method permits the programming realization which made possible its operative laboratorial usage.

Further development of the method assumes that the number of factors which were not treated here (for example, finite precision of the experimental data, ordinate of symmetry axis of discharge, etc.) has to be taken into consideration. However, everything that was mentioned becomes important after the wide testing of the presented method in the laboratorial practice.

References

[1] Griem HR. Plasma spectroscopy. New York: McGraw-Hill Book Company, 1963.

[2] Fleurier C, Chapelle J. Comput Phys Commun 1974;7:200–6.

[3] Zhovtiyancky VA, Babich IL, Veklich AN, Cheredarchuk AI. Inzh Fiz Zh 1998;71(1):131–8.